Applied Catalysis A: General 385 (2010) 136–143

Contents lists available at ScienceDirect

Applied Catalysis A: General

journal homepage: www.elsevier.com/locate/apcata

Selective vapour-phase α-pinene isomerization to camphene over gold-on-alumina catalyst

I.L. Simakova[a,*], Yu.S. Solkina[a,b], B.L. Moroz[a,b], O.A. Simakova[a,c], S.I. Reshetnikov[a], I.P. Prosvirin[a], V.I. Bukhtiyarov[a,b], V.N. Parmon[a,b], D.Yu. Murzin[c,*]

[a] G.K. Boreskov Institute of Catalysis SB RAS, Novosibirsk, Russia
[b] Novosibirsk State University, Russia
[c] Åbo Akademi University, Process Chemistry Centre, Turku/Åbo, Finland

ARTICLE INFO

Article history:
Received 26 April 2010
Received in revised form 22 June 2010
Accepted 3 July 2010
Available online 30 July 2010

Keywords:
Gold catalysts
Isomerization
α-Pinene
Camphene

ABSTRACT

The vapour-phase isomerization of α-pinene for the first time was studied over a supported Au catalyst. α-pinene was isomerized to camphene over the 2.2% Au/γ-Al_2O_3 catalyst at 463–483 K using a solution of the reagent in *n*-octane as the initial reaction mixture and H_2 or N_2 as a carrier gas. Under these conditions, the selectivity to camphene reaches 60–80% at 99.9% conversion of α-pinene. The reaction is found to be first-order with respect to α-pinene, the apparent activation energy being similar to that observed with the conventional TiO_2 catalyst. The prominent catalyst deactivation has been observed at increased α-pinene concentrations in the inlet reaction mixture (≥4 vol% in *n*-octane solution). According to HRTEM and TPO results, the deactivated catalyst contains the carbonaceous deposits that may block the catalyst surface. Almost complete regeneration was done in flowing O_2 at temperature up to 923 K required to totally eliminate the coke deposits.

1. Introduction

As it is known starting from classical Haruta's works [1], metallic gold particles with a size of several nanometers may exhibit high catalytic activity and/or unusual selectivity in numerous redox transformations of organic compounds [2–5]. Meanwhile, only a few examples of isomerization reactions catalyzed by supported gold including double bond migration in allylbenzene [6] or linoleic acid [7] and skeletal rearrangements (ring opening of propylene oxide to acetone [8], cycloisomerization of γ-acetylinic carboxylic acids [9] *etc.*) were communicated as yet. Herein, we report that the nanodispersed Au/γ-Al_2O_3 catalyst prepared by fairly simple procedure reveals good catalytic activity and selectivity for vapour-phase isomerization of α-pinene to camphene at 463–483 K with the use of H_2 or N_2 (1 bar) as a carrier gas. This reaction representing alkyl group migration from one carbon to a neighboring carbon (Wagner–Meerwein rearrangement) has high practical significance as a first step in the industrial synthesis of camphor from α-pinene which is the major constituent of turpentine [10,11]. In industry, the transformation of α-pinene into camphene is performed in liquid phase at 423–443 K over TiO_2 catalyst activated *in situ* by H_2SO_4 with rather low reaction rate obtaining yields from 35 to 50% [12,13]. Other catalysts mainly of acidic type such as natural [10,14–16] and synthetic zeolites [17–19], activated carbon [20], clays [21,22], ion exchange resins [11] and silica-supported rare earth oxides [23] were also examined in this reaction. To the best of our knowledge, supported gold metal catalysts have never been tested for α-pinene isomerization.

2. Experimental

2.1. Materials

Hydrogen tetrachloroaurate $HAuCl_4$·aq (49.47 wt% Au) was purchased from Aurat (Russia) and used without further purification. α-Pinene used for the catalytic tests was isolated from turpentine oil by vacuum distillation and contained the following impurities: tricyclene—0.19 wt%, camphene—1.61 wt%, β-pinene—3.54 wt%, 3-carene—1.30 wt%. *n*-Octane which is used as a solvent was purchased from Reakhim (Russia) and purified by vacuum distillation.

As a catalyst support, γ-alumina supplied by Ryazan Oil Refinery Company (Russia) was used in the form of 200–500 μm granules with S_{BET} of 268 $m^2\,g^{-1}$ and total pore volume of 0.69 $cm^3\,g^{-1}$. It was dried at 383 K in an oven for 8 h immediately before the catalyst preparation.

* Corresponding authors.
E-mail addresses: simakova@catalysis.ru (I.L. Simakova), dmurzin@abo.fi (D.Yu. Murzin).

0926-860X/$ – see front matter © 2010 Elsevier B.V. All rights reserved.
doi:10.1016/j.apcata.2010.07.002

2.2. Catalyst preparation

The method for preparing the Au/γ-Al_2O_3 catalyst was similar to those previously described [24]. A weighed amount of γ-Al_2O_3 was incipient wetness impregnated with an aqueous 0.06 M $HAuCl_4$ solution, the volume of the impregnating solution being 10% higher than the total pore volume of the support. The resulting paste was mixed for 1 h, allowed to stay in air at room temperature overnight and dried at 323 K for 8 h with the use of a vacuum system. Upon treatment in flowing H_2 at 673 K for 4 h, the sample was agitated with 2 portions of an aqueous 1 M NaOH solution (100 mL per 1 g sample) for removal of Cl^- impurity and neutralization of acidic sites on the support surface. After that, it was thoroughly washed with warm distilled water in order to remove Na^+ impurity and excess hydroxide ions. Finally, the sample was repeatedly dried as described above and calcined in air at 673 K for 4 h.

2.3. Characterization of catalyst

The Au and Cl contents of the catalyst were measured using X-ray fluorescence (XRF) technique on a VRA-30 instrument equipped with a Cr-anode. The diffuse reflectance UV–vis spectra were recorded on a Shimadzu UV-2501 PC spectrometer equipped with an ISR-240 integrating sphere attachment for diffuse reflectance measurements, using $BaSO_4$ as a reference, in the range of 200–1000 nm and presented in Kubelka–Munk function $F(R)$-wavelength coordinates. Transmission electron microscopy (TEM) studies were carried out on a JEOL JEM-2010 electron microscope operated at 200 kV and giving an information limit of 0.14 nm. The diameters of the Au crystallites were determined from TEM images taken with a medium magnification, at least 300 crystals being included in the particle size distribution for a sample. The temperature-programmed oxidation (TPO) of the catalyst samples was carried out on a NETZSCH STA 409PC instrument equipped with a quadrupole mass-spectrometer for determination of the composition of oxidation products. The sample placed on a thermobalance was heated in flowing air (40 $cm^3\ min^{-1}$) at 323 K for 1 h, and thereafter the temperature was raised to 923 K for 1 h (ramping 10 K min^{-1}).

Photoelectron spectra were recorded using SPECS spectrometer with PHOIBOS-150 hemispherical energy analyzer and MgK_α irradiation ($h\nu$ = 1253.6 eV, 100 W). Binding energy scale was preliminarily calibrated by the position of the peaks of $Au4f_{7/2}$ (84.0 eV) and $Cu2p_{3/2}$ (932.67 eV) core levels. For recording of spectra the samples were supported to the conductive scotch tape. The binding energy of peaks was corrected to take into account the sample charging by referencing to the Al2p (74.5 eV) (internal standard). This reference was applied since the spectrometer was equipped with turbomolecular pumps, and calibration on the basis of the position of C1s core level, typically used in the case of vacuum systems with diffusion pumps, was difficult. The ratio of surface atomic concentrations of the elements was calculated from the integral intensities of photoelectron peaks corrected by corresponding atomic sensitivity factors (ASF). In addition to the survey photoelectron spectra, more narrow spectral regions Al2p, Au4f, Al2s, C1s, and O1s have been recorded. For the survey spectra the pass energy of the analyzer was 50 eV, while for the narrow spectral regions the pass energy was 10 eV.

2.4. Isomerization procedure

Vapour-phase isomerization of α-pinene was carried out under continuous flow conditions at atmospheric pressure using a solution of α-pinene in *n*-octane of the determined concentration as the initial reaction mixture and H_2 or N_2 as a carrier gas. Just before mixing with α-pinene vapour, H_2 or N_2 were deoxidized and dried by passing successively through the columns filled with a reduced Ni-Cr catalyst and silica. A catalyst sample (200 mg) was placed in a U-shaped glass plug-flow reactor of 4 mm i.d. equipped with a thermocouple which was fixed in the middle of the catalyst bed outside the reactor tube. The carrier gas was passed through the catalyst bed at the desired space velocity (SV), and the temperature was raised up to 463–483 K. Then α-pinene solution in *n*-octane was supplied via a heated pre-chamber of U-reactor to be vapourized and mixed with the carrier gas before passing to the catalyst bed. The residence time (τ) in the reactor was fixed by controlling SV of the carrier gas within the range of 1600–14500 h^{-1}. The samples (100–200 μL) of the outlet gas stream were taken into a condenser connected to the effluent tube of the reactor. The products were identified by GC–MS (Agilent 6890, the quartz capillary column 50 m/0.2 mm/0.5 μm, SE-30). The contents of the inlet and outlet reaction mixtures were analyzed by a gas chromatograph («Tzvet-500») equipped with a flame-ionization detector and a capillary Carbowax-20 M column (50 m/0.2 mm/0.5 μm). The column was hold at 393 K, both injection inlet and detector temperatures were 473 K. The conversion of α-pinene, X(%), and the selectivity, S(%), to the determined product were calculated, using the corresponding equations below:

$$X(\%) = \frac{[\alpha\text{-pinene}]_{inlet} - [\alpha\text{-pinene}]_{outlet}}{[\alpha\text{-pinene}]_{inlet}} \times 100$$

$$S(\%) = \frac{[product]_{outlet}}{[\alpha\text{-pinene}]_{inlet} - [\alpha\text{-pinene}]_{outlet}} \times 100$$

During all tests, the carbon balance between the feed and outlet stream was within 100 ± 5%.

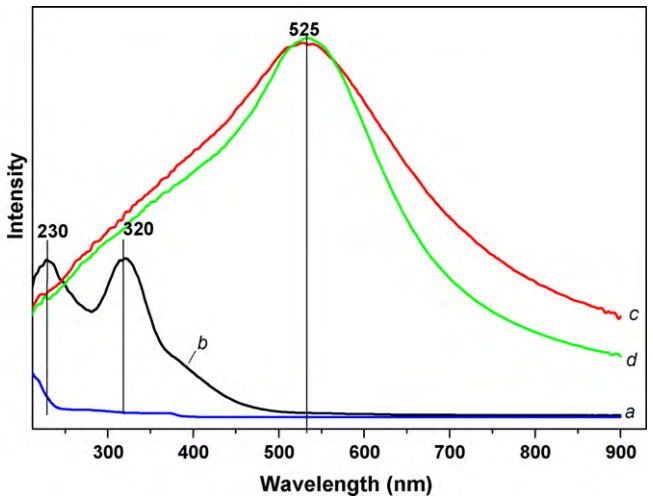

Fig. 1. Diffuse reflectance UV–vis spectra: (a) γ-Al_2O_3 support lacking gold; (b) γ-Al_2O_3 after impregnation with $HAuCl_4$ solution and drying; (c) sample b after reduction with H_2 at 673 K; (d) sample c treated with 1 M NaOH and calcined in air at 673 K.

3. Results and discussion

3.1. Characterization of catalyst

The impregnation of γ-alumina with an aqueous $HAuCl_4$ solution followed by drying produced yellow samples which turned to dark violet upon calcination in a H_2 flow at 673 K. The loading of Au was 2.2 wt%, as determined by XRF.

Fig. 1 shows the diffuse reflectance UV–vis spectra of the Au/γ-Al_2O_3 catalyst at different stages of its preparation. The spectrum of γ-Al_2O_3 after impregnation with the $HAuCl_4$ solution exhibits

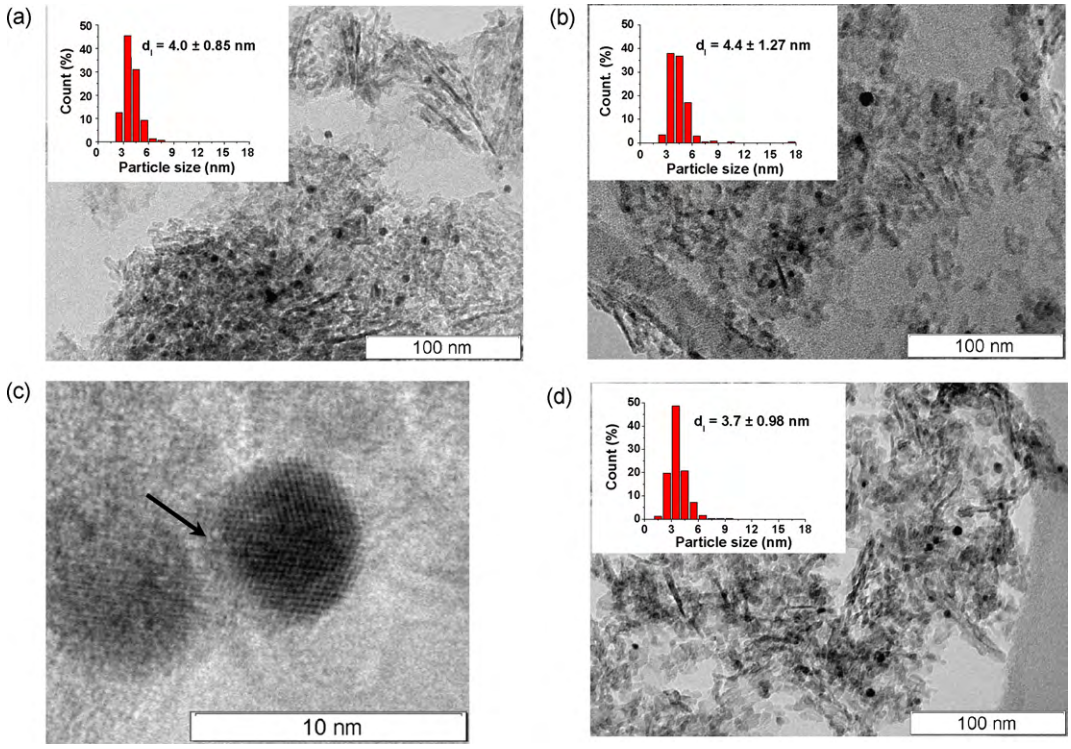

Fig. 2. TEM images of the 2.2% γ-Al_2O_3 catalyst: (a) as-prepared catalyst; (b) the catalyst after testing for α-pinene isomerization at 473 K and $[\alpha\text{-pinene}]_{inlet}$ = 20 vol%; (c) HRTEM image of Au particle located at the surface of the spent catalyst (the arrow indicates the layer of disordered structure covering the surface of Au particles); (d) sample b after TPO in flowing air at 323 K for 1 h and thereafter during the temperature rise up to 923 K (heating rate 10 K min^{-1}). The insets in (a), (b) and (d) show Au particle size distributions in the samples.

strong, broadened absorption bands at 230 and 320 nm, belonging to $[AuCl_4]^-$ complexes. Subsequent treatment of the sample with H_2 results in the appearance of the strong band at 525 nm derived from the plasmon absorption by Au^0 nanoparticles [25]. Simultaneously, the absorption bands at 230 and 320 nm disappear from the spectrum. Washing with an aqueous 1 M NaOH solution followed by calcination in air at 673 K leads neither to gold leaching from the reduced sample nor to significant changes in the UV–vis spectrum, but allows the Cl content to be decreased by an order of magnitude (from 5000 to 100–200 ppm), according to XRF data. From the TEM data shown in Fig. 2a, the final Au/γ-Al_2O_3 catalyst comprises both small (d_i < 5 nm) and relatively large (d_i = 5–8 nm) Au^0 particles, while the former predominate in the number and weight fraction. Particle sizes of the sample are fitted well by the lognormal distribution with the maximum at around 4 nm (mean linear diameter (d_l) is equal to 4.0 ± 0.85 nm).

The XPS results of Au4f spectra for the fresh catalyst, the crushed fresh catalyst and the catalyst after reaction are shown in Fig. 3. For the samples the binding energy of $Au4f_{7/2}$ was 83.9 eV, which was assigned to metallic gold. $Au4f_{7/2}$ binding energy value is typical for metallic gold particles supported on various oxide carriers [26]. The Au/Al atomic ratio measured for the fresh Au/γ-Al_2O_3 sample (0.022) does not evidence any change after crushing (0.021) and the reaction (0.022), which is an indication of gold homogeneity along support particle radius at least above 1 μm, which is the size of grinded catalysts. The fact that no peaks are observed in the E_b region of 84.5–88 eV characteristic of "ionic" gold species can be accounted for by the rapid reduction of Au(III) or Au(I) species, if any are contained in the sample, under the action of photoelectron beam during recording the XP spectra [24]. The results of XPS indicated that the major fraction of the gold species on the catalyst surface is metallic gold, with a minor fraction of gold species that can be attributed to an oxidized state (Au^+) which is coordinated with OH-groups [24].

3.2. Catalytic performance

Table 1 presents the results obtained with the nanosized 2.2% Au/γ-Al_2O_3 catalyst in vapour-phase isomerization of α-pinene at 473 K and low reagent concentration in the inlet *n*-octane solution ($[\alpha\text{-pinene}]_{inlet}$ = 0.4 vol%) under H_2 atmosphere. Under these conditions, the gold catalyst exhibits high activity for α-pinene isomerization, the α-pinene conversion being not significantly changed during the whole testing run (typically, for 7–8 h) (Entries 1 and 2). At the residence time of 0.33 s (SV = 2200 h^{-1}) the α-pinene conversion reached 99.9% with fairly good and stable selectivity to camphene (*S* = 65.5%), the rest of the products were mainly

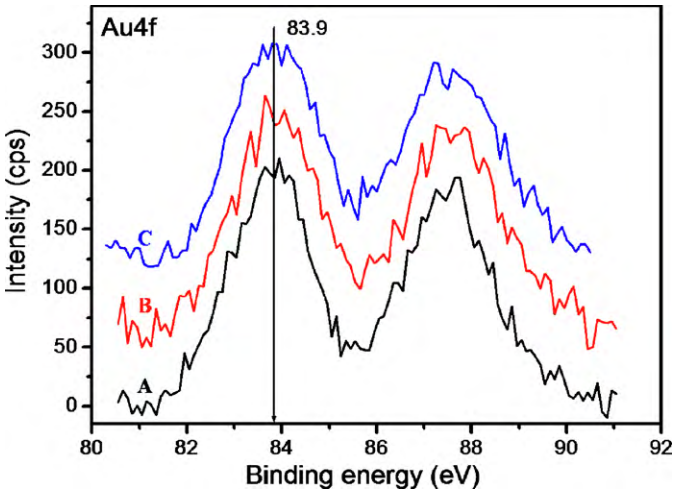

Fig. 3. XP spectra of Au4f region of a 2.2 wt% Au/Al_2O_3 catalyst: (a) before reaction, (b) after reaction, and (c) crushed catalyst before reaction.

Table 1
Results of vapour-phase α-pinene isomerization over the 2.2 wt% Au/γ-Al_2O_3 catalyst (in comparison with γ-Al_2O_3 lacking gold).[a].

Entry	Catalyst	Total conversion (%)	Selectivity (%)				
			Camphene	Limonene	*p*-Cymene	Tricyclene	Others
1	Au/γ-Al_2O_3	99.9	65.5	1.2	14.6	8.2	10.5
2[b]	Au/γ-Al_2O_3	99.9	66.3	1.5	14.1	8.3	9.8
3[c]	Au/γ-Al_2O_3	99.8	66.2	1.8	14.0	7.7	10.3
4	γ-Al_2O_3[d]	2.7	28.3	14.6	11.1	16.8	29.2

[a] Reaction conditions: $[\alpha\text{-pinene}]_{inlet}$ 0.4 vol%, solvent *n*-octane, catalyst 0.2 g, 473 K, H_2 atmosphere, SV 2200 h^{-1}, 1 h.
[b] In 6 h after the beginning of the catalytic run.
[c] Tested with the use of N_2 as a carrier gas.
[d] Impregnated with 0.01 M HCl solution, outgassed at 323 K, calcined in a H_2 flow at 673 K for 4 h, then washed with 1 M NaOH and distilled water, outgassed at 323 K and, finally, calcined in air at 673 K for 4 h.

p-cymene and tricyclene (S = 14.5 and 8.2%). Even at τ of 0.05 s that was the minimum τ value possible during our testing procedure, α-pinene conversion remains too high in order to measure the reaction rate under differential conditions. The replacement of H_2 as a carrier gas by N_2 does not cause any considerable changes in the α-pinene conversion and product distribution (Entry 3). A blank experiment (Entry 4) was done with γ-Al_2O_3 lacking gold but subjected to the same kind of chemical and thermal treatment that was used at different stages of the gold catalyst preparation (except that a solution of 0.01 M HCl was taken instead of $HAuCl_4$ solution for γ-alumina impregnation). As a result, only very low conversion (X = 2.7%) was observed with a wide product distribution in which camphene and limonene were the main products (S = 28.3 and 14.6%). The data obtained suggest that, firstly, the vapour-phase α-pinene isomerization reaction proceeds on the Au/γ-Al_2O_3 catalyst without chemical participation of H_2 and, secondly, the gold is necessary for the catalysis.

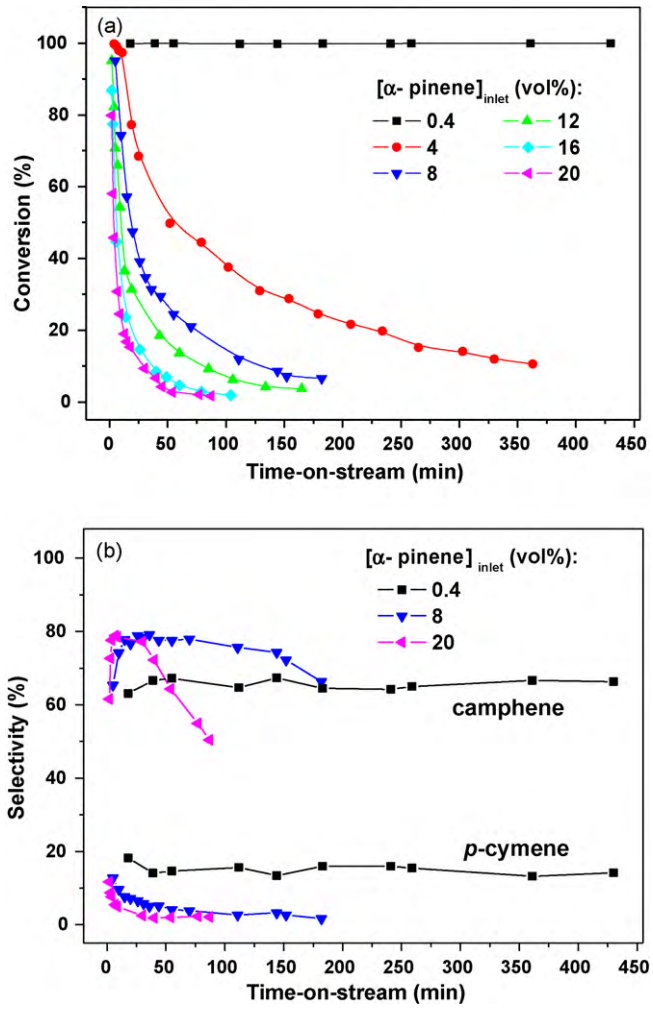

Fig. 4. Time dependence of α-pinene conversion (a) and selectivity to camphene and *p*-cymene (b) over the 2.2% Au/γ-Al_2O_3 catalyst at various concentrations of α-pinene in the inlet *n*-octane solution. Reaction conditions: temperature 473 K, catalyst 200 mg, carrier gas H_2, SV 2200 h^{-1}.

Fig. 4 shows the results of α-pinene isomerization over the Au/γ-Al_2O_3 catalyst at various $[\alpha\text{-pinene}]_{inlet}$ values. It is clearly seen that increasing α-pinene concentration in the inlet reaction mixture by a factor of 10 induces the prominent deactivation of the catalyst, the deactivation rate rising sharply with a further increase in the reagent concentration (Fig. 4a). At $[\alpha\text{-pinene}]_{inlet} \geq 4$ vol%, selectivity to camphene during the initial period of testing arises to ca. 80% that apparently is related to a drop in α-pinene conversion, but then decreases notably with time-on-stream along with the catalyst activity (Fig. 4b). Initial period of α-pinene isomerization does not represent a single value being dependent on pinene concentration (ca. 1–5 min). During this time approximately the same amount of α-pinene passed through the catalyst bed (e.g. for higher pinene concentration the initial period was lower) in order to assure that sampling times correspond to approximately the same extent of deactivation.

The effects of residence time and temperature on α-pinene isomerization over Au catalyst were further studied at the highest concentration of the reagent ($[\alpha\text{-pinene}]_{inlet}$ = 20 vol%), which was used in this work. Fig. 5a displays α-pinene conversion measured during the initial period of testing versus τ for three different reaction temperatures. The experimental data are well described by the equation:

$$X = 1 - e^{-k\tau}, \quad (1)$$

where X is conversion and k is the rate constant. This indicates the reaction is first-order with respect to α-pinene. The k values for different reaction temperatures determined by fitting the experimental data to Eq. (1) are presented in Table 2. Plotting the graph of $\ln(k)$ versus $1/T$ results in a straight line, as shown in Fig. 5b. The apparent activation energy, E_a, for α-pinene isomerization over the 2.2 wt% Au/γ-Al_2O_3 catalyst (within the temperature range from 463 to 483 K) calculated from the slope of Arrhenius plot is 51.0 kJ mol^{-1} (with 95% confidence limits). This value is close

Table 2
First-order reaction rate constants (with 95% confidence limits) for α-pinene isomerization over the 2.2 wt% Au/γ-Al_2O_3 catalyst at different temperature.[a].

Temperature (K)	Rate constant, k (s^{-1}), and deviation
463	3.60 ± 0.10
473	4.75 ± 0.10
483	6.24 ± 0.12

[a] Reaction conditions: $[\alpha\text{-pinene}]_{inlet}$ 20 vol%, solvent *n*-octane, catalyst 0.2 g, H_2 atmosphere, residence time 0.05–0.45 s.

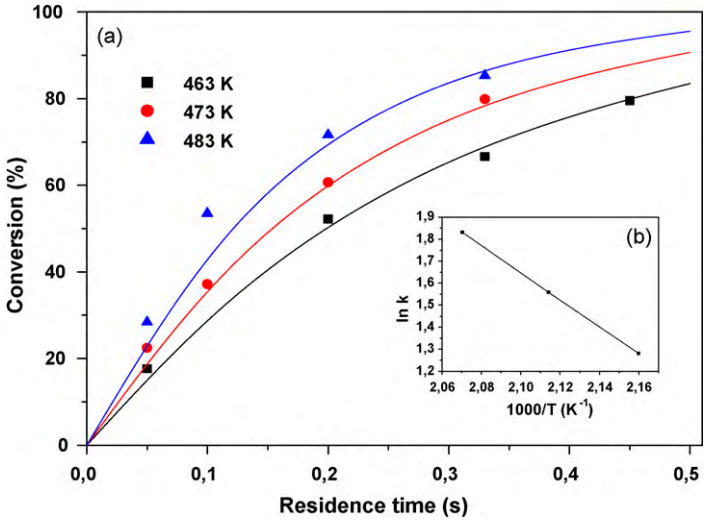

Fig. 5. (a) Conversion of α-pinene during the initial period of reaction over the 2.2% Au/γ-Al_2O_3 catalyst as a function of residence time for different temperatures. The symbols represent the experimental data, while the lines represent the model fit to the experimental data. (b) Arrhenius plot of rate constant (k, s^{-1}) of α-pinene isomerization. Reaction conditions: $[\alpha\text{-pinene}]_{inlet}$ 20 vol%, solvent n-octane, catalyst 200 mg, carrier gas H_2.

to the one obtained for α-pinene isomerization over TiO_2 catalyst (46.1 kJ mol^{-1}) [27], which suggests that the rate-determining steps are similar in both cases.

Fig. 6 presents selectivity to the main products measured during the initial period of α-pinene isomerization over the Au/γ-Al_2O_3 catalyst at high reagent concentration ($[\alpha\text{-pinene}]_{inlet}$ = 20 vol%) as a function of the reagent conversion for different reaction temperatures. Selectivity to camphene, *p*-cymene and tricyclene varies little with conversion indicating that these products are formed in parallel pathways. It is in a good agreement with the conventional reaction mechanism suggested for α-pinene isomerization over acid catalysts [15,21], which is shown in Scheme 1. According to this, pinylcarbonium ion that is initially formed from α-pinene is the general precursor of all the reaction products. It is further rearranged into bornylcarbonium and terpenilcarbonium ions, the former giving camphene and tricyclene in parallel steps, while the latter leading to *p*-cymene and limonene in parallel steps too. In fact, selectivity to limonene changes with conversion stronger (from 17.6 to 1.6%) than selectivity to other main products of α-pinene isomerization, but it may result from subsequent polymerization with the formation of high molecular weight compounds, which are not detected by GC. Such preferential oligomerization/polymerization of limonene could be explained by the presence of the terminal double bond. It is also seen from Fig. 6 that the selectivity to camphene, *p*-cymene, tricyclene and limonene over Au catalyst does not depend on reaction temperature, at least, in the range of 463–483 K. Thus, the apparent activation energies for their formation are approximately the same and, therefore, the difference in the rate constants for the formation of various products is probably due to the difference in the activation entropies.

At present, the reason for high activity and selectivity of the Au/γ-Al_2O_3 catalyst in α-pinene isomerization to camphene cannot be elucidated mainly due to the lack of available information on the nature of the active site. However, taking into account that cationic gold(I) complexes have recently evolved as

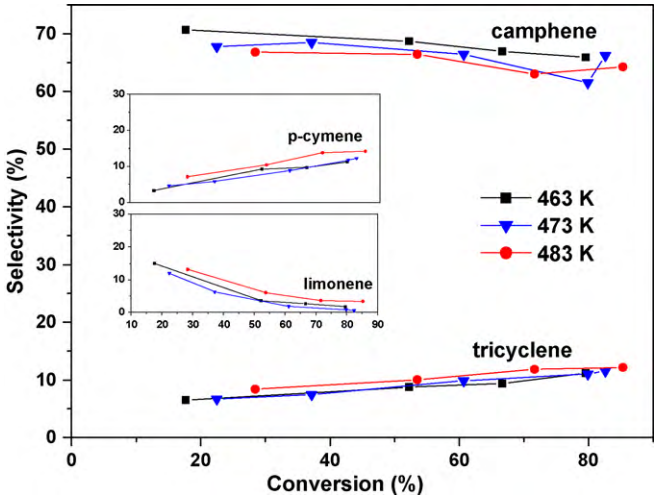

Fig. 6. Selectivity to significant products during the initial period of α-pinene isomerization over the 2.2 wt% Au/γ-Al_2O_3 catalyst as a function of the reagent conversion for different reaction temperatures. The reaction conditions: $[\alpha\text{-pinene}]_{inlet}$ 20 vol%, solvent n-octane, catalyst 200 mg, carrier gas H_2, residence time 0.05–0.45 s.

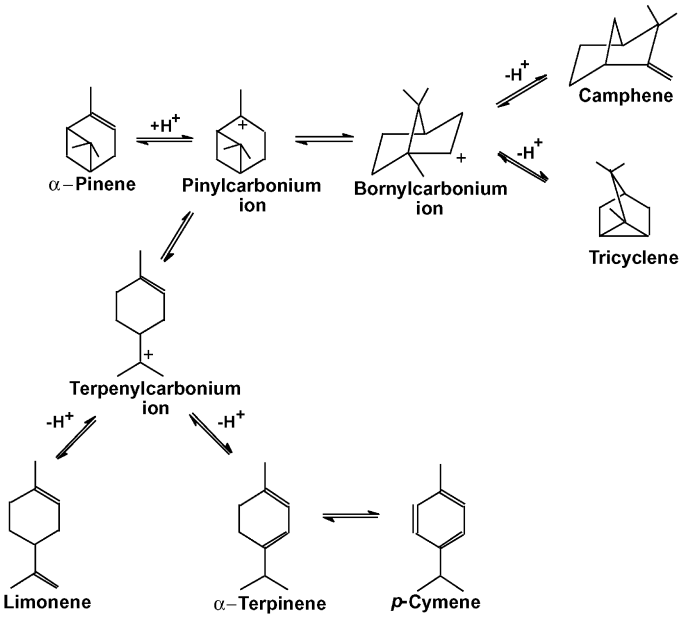

Scheme 1. Mechanism of α-pinene isomerization over acid catalysts.

excellent Lewis acid catalysts for various Wagner–Meerwein shifts such as the ring expansion of cyclopropanols to the corresponding cyclobutanones [28,29], participation of Au^+ species in the catalytic cycle of α-pinene isomerization over the Au/Al_2O_3 catalyst can be hypothesized; even though they were not detected by XPS in the present study. Application of XPS did not allow to detect Au cations because Au particle sizes in the investigated catalysts are about 3–5 nm (TEM), which is comparable with the depth of XPS beam penetration. It means that $Au4f_{7/2}$ intensity corresponds to total concentration of metallic Au. Obviously it is difficult by XPS to reveal relatively small amounts of Au cations in comparison with much larger amounts of metallic Au even if Au cations are indeed present in the sample.

Au^+ species were presumed [24,30–32] to be present on the surface together with the gold in the metallic state. In particular in [24] it was demonstrated (including also catalysts used in the current work), that regardless of the preparation techniques catalysts contained metallic Au particles together with the surface ionic Au oxide species. Other authors using FTIR spectroscopy of adsorbed CO also showed that heating of reduced metallic gold in oxygen at 673 K leads to formation of a small fraction of Au^+ sites isolated on the support and oxidation of the gold atoms on the surface of the gold particles to Au^+ [33]. In the current work $Au/\gamma\text{-}Al_2O_3$ catalyst was not studied by FTIR spectroscopy of adsorbed CO, however, the catalyst was treated at conditions comparable with [33]: under reducing atmosphere at the temperature of 673 K for 4 h followed by oxidizing at the temperature of 673 K for 4 h.

The role of cationic and metallic Au was discussed in [34] where a unique role of cationic interfacial gold species has been proposed. The elegant experiments of Fu et al. [35] revealed the critical role of cationic gold in the water–gas shift reaction. The authors deposited gold onto a La-doped cerium oxide support by either deposition precipitation or co-precipitation and then calcined the material in air at 400 °C. Most of the gold was reduced to metallic particles by the thermal treatment. A basic sodium cyanide solution was then used to leach the metallic gold from the catalyst surface in a process similar to gold extraction during mining. X-ray photoelectron spectroscopy showed that in a co-precipitated sample, the gold remaining on the support after leaching was exclusively ionic. Although the leaching process removed 85% of the gold, the catalytic activity per surface area was unaffected by the loss of metallic particles. These results suggest that ionic gold strongly interacts with the support and is the active site for the reaction.

3.3. Catalyst deactivation and regeneration

TEM study of the spent $Au/\gamma\text{-}Al_2O_3$ catalyst demonstrated that the mean linear diameter of Au particles does not significantly change during α-pinene isomerization at 473 K and $[\alpha\text{-pinene}]_{inlet}$ = 20 vol% (*cf.* Fig. 2a and b). Generally, gold particles of 3–6 nm in diameter are observed both before and after testing, even though the particle size distribution of the spent catalyst is found to be somewhat broader due to appearance of few larger Au particles with the sizes between 10 and 20 nm. Nevertheless, it seems that sintering of metal particles is not the main reason for the deactivation of the catalyst. At the same time, in the micrographs of the spent $Au/\gamma\text{-}Al_2O_3$ catalyst recorded under the high-resolution (HR) conditions (Fig. 2c) the surface of the Au crystallites was seen to be covered with a thin (subnanometer) layer of disordered structure. The HRTEM images of these overlayers exhibit very low contrast, indicating that relatively light atoms (such as carbon) are exclusively present in the overlayer. A similar layer seemingly covers the Al_2O_3 surface as can be suggested on the basis of low contrast and high fuzziness of the TEM picture observed with the spent catalyst in comparison with the fresh one.

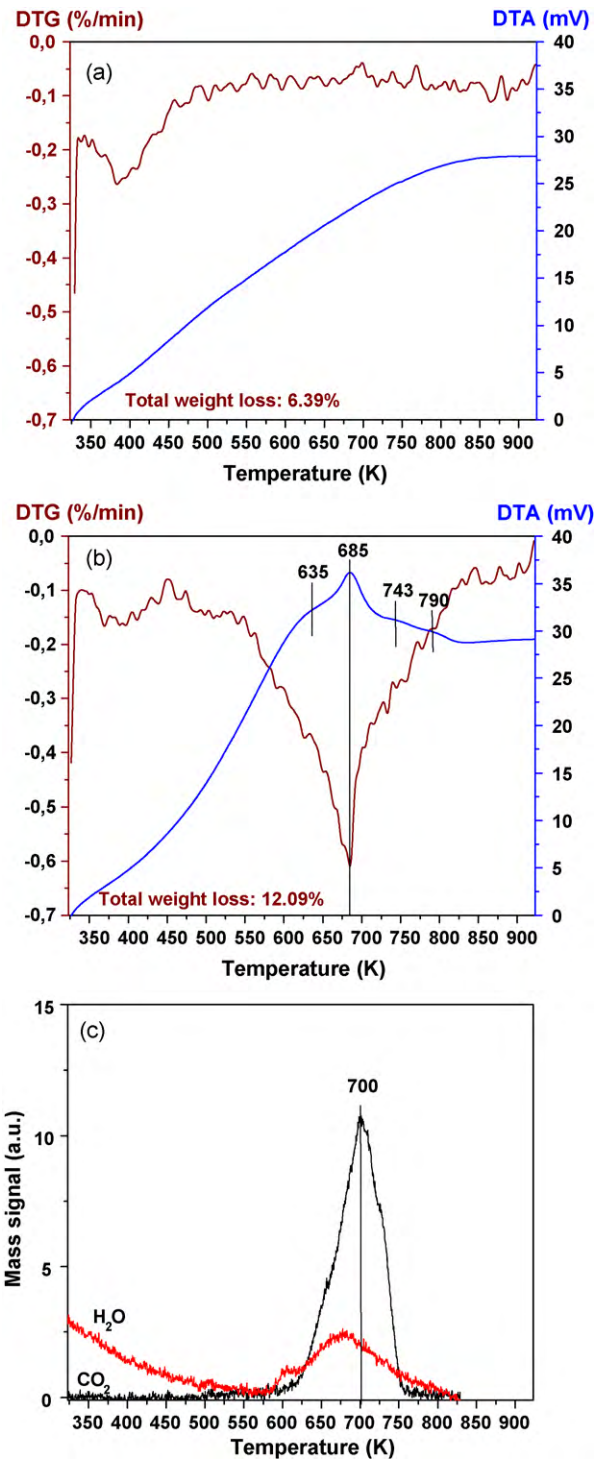

Fig. 7. DTG/DTA curves of (a) as-prepared and (b) spent $Au/\gamma\text{-}Al_2O_3$ catalyst during TPO in flowing air at heating rate 10 K min^{-1}. (c) The outlet product pressure profiles during TPO of the spent $Au/\gamma\text{-}Al_2O_3$ catalyst.

Fig. 7 displays the results of a TPO study on the 2.2 wt% $Au/\gamma\text{-}Al_2O_3$ catalyst before and after vapour-phase α-pinene isomerization, which was carried out in the equipment for thermogravimetric and differential thermal analysis (TGA and DTA, respectively). The differential thermogravimetric (DTG) curve of the fresh catalyst (Fig. 7a) exhibits broad peaks at 385 and >800 K. The former one is related, most probably, to removal of adsorbed water, while the latter can be assigned to elimination of OH groups from the alumina surface (total loss of the sample weight during

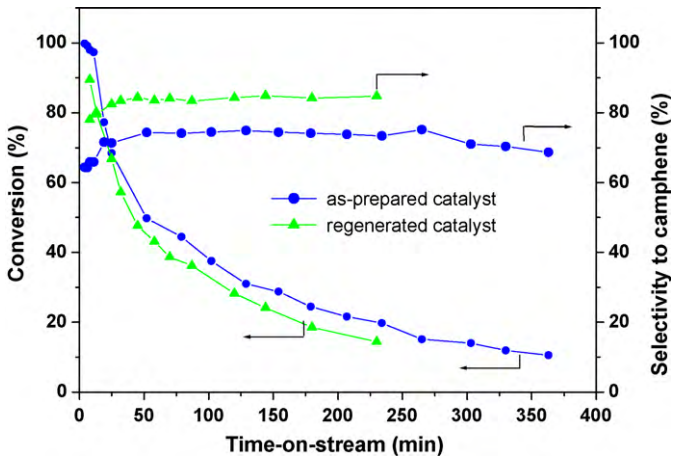

Fig. 8. Time dependence of α-pinene conversion and selectivity to camphene over the 2.2% Au/γ-Al_2O_3 catalyst taken as-prepared and after regeneration in flowing O_2 at 323–923 K (heating rate 10 K min^{-1}). Reaction conditions: temperature 473 K, $[\alpha\text{-pinene}]_{inlet}$ 4 vol%, solvent *n*-octane, catalyst 200 mg, carrier gas H_2, residence time 0.33 s.

TPO is 6.39%). The DTA curve of the fresh sample shows no signs of any exothermal reaction. For the spent catalyst, the DTG curve measured under TPO conditions (Fig. 7b) contains additionally the peak at 685 K that corresponds to loss of 5.42% of the sample weight. Simultaneously, the DTA curve of the spent catalyst shows the overlapping exhothermic peaks at 635, 685, 745 and 790 K, the most distinct peak coinciding with the maximum weight loss observed by means of TGA equipment. This may be attributed to combustion of carbonaceous species deposited onto the catalyst surface. Indeed, the formation of CO_2 as the main oxidation product during TPO of the spent Au/γ-Al_2O_3 catalyst was observed by means of mass spectrometry (Fig. 7c) starting from 625 K up to about 775 K with a maximum at 700 K. Along with CO_2, the traces of H_2O appear with a maximum yield at 682 K, indicating that the exhothermic peaks at 635 and 685 K are related to oxidation of hydrogen-enriched carbonaceous species deposited onto the catalyst surface, whereas the exhothermic peaks at 745 and 790 K are caused by surface carbon (coke) combustion. One can suggest that coke is formed on the catalyst surface owing to adsorption of α-pinene and its isomers followed by their oligomerization and secondary transformations of the oligomers. Apparently, deposition of carbonaceous species blocks the active sites of the Au/γ-Al_2O_3 catalyst being the main reason for the catalyst deactivation. The rate of coke formation should decrease as α-pinene concentration in the inlet reaction mixture decreases. Probably, this is the reason the gold catalyst to show stable activity at α-pinene concentration of 0.4 vol%, at least, for 7–8 h.

As shown in Fig. 2d, TPO of the spent catalyst in flowing air conducted up to 923 K restores high contrast and sharpness of TEM images of the catalyst surface, but has no considerable effect on the mean Au particle size and size distribution. This is in agreement with the previous observations of very high resistance of alumina-supported gold nanoparticles against sintering, probably, caused by the epitaxial interaction between Au crystallites and alumina surface with the formation of Au–O–Al bonds [32,36,37].

The high sintering stability of Au/γ-Al_2O_3 catalyst used in this work provides the possibility of restoring its activity in α-pinene isomerization by burning the carbonaceous species deposited onto the catalyst surface at temperatures ≥800 K that are required for coke burning, as follows from TPO experiments. In order to check this assumption, the deactivated catalyst was calcined in a quartz flow reactor with an O_2 flow (40 cm^3 min^{-1}) initially at 323 K for 1 h, then during the temperature rise up to 923 K with a constant heating rate of 10 K min^{-1} and cooled down to 298 K in flowing O_2. Thereafter the catalyst was allowed to stay at room temperature for 12 h before measuring is catalytic activity. Fig. 8 demonstrates that such kind of treatment restores α-pinene conversion over the gold catalyst at 473 K, $[\alpha\text{-pinene}]_{inlet}$ = 4 vol% and τ = 0.33 s up to 90% of its initial value, while selectivity to camphene even increased from ca. 70 to ca. 80%.

4. Conclusion

In summary, this work demonstrates for the first time that the nanodispersed Au/γ-Al_2O_3 catalyst, prepared from $HAuCl_4$ as a gold precursor by impregnation procedure including treatment of the reduced sample with NaOH for neutralization of acidic sites on the support surface, shows good catalytic activity and selectivity for vapour-phase isomerization of α-pinene to camphene at 463–483 K with the use of H_2 or N_2 (1 bar) as a carrier gas. Activity significantly exceeded the catalytic performance of neat Al_2O_3 pretreated with NaOH, which indicates that gold is necessary for this kind of Wagner–Meerwein skeletal rearrangements. At low α-pinene concentration in the inlet reaction mixture α-pinene conversion over Au/γ-Al_2O_3 catalyst is not significantly changed during the catalytic run, at least, for 7–8 h. However, increasing α-pinene concentration in the inlet reaction mixture induces the intense deactivation of the catalyst. HRTEM and TPO results show that deposition of carbonaceous species, which may block the active sites of the Au/γ-Al_2O_3 catalyst, is the main reason for the catalyst deactivation. The calcination of the deactivated catalyst in flowing O_2 at temperatures up to 923 K restores its activity and selectivity in α-pinene isomerization to camphene almost completely. In an ongoing study, we are optimizing the composition and conditions of preparation of gold catalysts for this reaction and elucidating the reason for high activity and selectivity of supported gold in isomerization of α-pinene to camphene.

Acknowledgements

The authors are grateful to Tatiana V. Larina, Eugene Yu. Gerasimov, George A. Filonenko, Irina L. Kraevskaya and Pavel A. Pyrjaev for their help in carrying out this work. This project is supported by the Russian Foundation for Basic Research (grants nos. 08-03-91758 and 09-03-12272). One of the authors (Yu.S.) acknowledges the financial support from the Foundation for Assistance to Small Innovative Enterprises.

References

[1] M. Haruta, Catal. Today 36 (1997) 153–166.
[2] G.C. Bond, C. Louis, D.T. Thompson, Catalysis by Gold, IC Press, London, 2006.
[3] P. Claus, Appl. Catal. A 291 (2005) 222–229.
[4] B. Grzybowska-Swierkosz, Catal. Today 112 (2006) 3–7.
[5] D.T. Thompson, Nanotoday 2 (2007) 40–43.
[6] V.V. Smirnov, S.A. Nikolaev, G.P. Murav'eva, L.A. Tyurina, A.Yu. Vasil'kov, Kinet. Catal. 48 (2007) 265–270.
[7] O.A. Simakova, A.-R. Leino, B. Campo, P. Mäki-Arvela, K. Kordás, J.-P. Mikkola, D.Yu. Murzin, Catal. Today 150 (2010) 32–36.
[8] A. Fasi, I. Palinco, K. Hernadi, I. Kirisci, Catal. Lett. 81 (2002) 237–240.
[9] F. Neatu, P.Y. Toulic, V. Michelet, V. Parvulescu, Pure Appl. Chem. 81 (2009) 2387–2396.
[10] F. Özkan, G. Gündüz, O. Akpolat, N. Beşün, D.Yu. Murzin, Chem. Eng. J. 91 (2003) 257–269.
[11] O. Chimal-Valencia, A. Robau-Sanchez, V. Collins-Martinez, A. Aguilar-Elguezabal, Biores. Technol. 93 (2004) 119–123.
[12] K.A.D. Swift, Top. Catal. 27 (2004) 143–155.
[13] P. Maki-Arvela, B. Holmbom, T. Salmi, D.Yu. Murzin, Catal. Rev. 49 (2007) 197–340.
[14] A.I. Allahverdiev, S. Irandoust, D.Yu. Murzin, J. Catal. 185 (1999) 352–362.
[15] A.I. Allahverdiev, B. Andersson, D.Yu. Murzin, Appl. Catal. A: Gen. 198 (2000) 197–206.
[16] O. Akpolat, G. Gündüz, F. Özkan, N. Beşün, Appl. Catal. A: Gen. 265 (2004) 11–22.

[17] A.D. Stefanis, G. Perez, A.A.G. Tomlinson, Appl. Catal. A: Gen. 132 (1995) 353–365.
[18] A. Severino, A. Esculcas, J. Rocha, J. Vital, L.S. Lobo, Appl. Catal. A: Gen. 142 (1996) 255–278.
[19] C.M. Lopez, F.J. Machado, K. Rodriguez, B. Mondez, M. Hasegawa, S. Pekerar, Appl. Catal. A: Gen. 173 (1998) 75–85.
[20] C.B. Davis, J.J. McBride, US Patent 3,824,135 (1974).
[21] G.A. Rudakov, Chemistry and Technology of Camphor, Lesnaya promyshlennost', Moscow, 1976 (in Russian).
[22] S. Kullaj, Bull. Shkencave Nat. 43 (1989) 81–85.
[23] T. Yamamoto, T. Matsuyama, T. Tanaka, T. Funabiki, S. Yoshida, J. Mol. Catal. 155 (2000) 43–58.
[24] B.L. Moroz, P.A. Pyrjaev, V.I. Zaikovskii, V.I. Bukhtiyarov, Catal. Today 144 (2009) 292–305.
[25] A.B.P. Lever, Inorganic Electronic Spectroscopy, second ed., Elsevier, Amsterdam, 1984.
[26] J.F. Moulder, W.F. Stickle, P.E. Sobol, K.D. Bomben, in: J. Chastain (Ed.), Handbook of X-Ray Photoelectron Spectroscopy, Perkin-Elmer, Eden Prairie, Minnesota, 1992.
[27] F. Ebmeyer, J. Mol. Struct. (Theochem.) 582 (2002) 251–255.
[28] F. Kleinbeck, F.D. Toste, J. Am. Chem. Soc. 131 (2009) 9178–9179 (and references therein).
[29] S.G. Sethofer, S.T. Staben, O.Y. Hung, F.D. Toste, Org. Lett. 10 (2008) 4315–4318.
[30] G.C. Bond, D.T. Thompson, Gold Bull. 33 (2000) 41–50.
[31] H.-S. Oh, C.K. Costello, C. Cheung, H.H. Kung, M.C. Kung, Stud. Surf. Sci. Catal. 139 (2001) 375–381.
[32] B.L. Moroz, D.A. Zyuzin, V.I. Zaikovskii, A.N. Shmakov, P.A. Pyrjaev, E.M. Moroz, V.I. Bukhtiyarov, Extended abstracts of the 9th European Conference on Catalysis "Catalysis for a Sustainable World" (EuropaCat IX), Salamanca, Spain, 2009, pp. P10–108.
[33] Tz. Venkov, Hr. Klimev, M.A. Centeno, J.A. Odriozola, K. Hadjiivanov, Catal. Commun. 7 (2006) 308–313.
[34] R.J. Davis, Science 301 (2003) 926–927.
[35] Q. Fu, H. Saltsburg, M. Flytzani-Stephanopoulos, Science 301 (2003) 935.
[36] B.L. Moroz, P.A. Pyryaev, V.I. Zaikovskii, S.Ph. Ruzankin, T.V. Larina, V.F. Anufrienko, V.I. Bukhtiyarov, in: V.N. Parmon, V.I. Bukhtiyarov, Z.R. Ismagilov (Eds.), Proceeding from the III International Conference "Catalysis: Fundamentals and Application", Part I, Boreskov Institute of Catalysis, Novosibirsk, 2007, p. 140.
[37] S. Ivanova, C. Petit, V. Pitchon, Gold Bull. 39 (2006) 3–8.